INORGANIC CHEMISTRY
FRONTIERS

RESEARCH ARTICLE

View Article Online
View Journal | View Issue

Cite this: *Inorg. Chem. Front.*, 2023, **10**, 6005

Deuteration of Pd-activated C(sp^2)–H bonds in the solid state†

Alen Bjelopetrović, ‡[a] Dajana Barišić, ‡[a,b] Marina Juribašić Kulcsár, *[a] Ivan Halasz, [a] Manda Ćurić[a] and Stipe Lukin *[a]

Received 19th May 2023,
Accepted 29th August 2023

DOI: 10.1039/d3qi00932g

rsc.li/frontiers-inorganic

We report mechanochemically-induced deuteration of Pd-activated aromatic C(sp^2)–H bonds at ambient temperature under solvent-free conditions. Deuterium was sourced from cysteine-d_4 to obtain mono- or dideuterated products from various aromatic palladacycles. Next to good deuteration yields, based on time-resolved *in situ* Raman monitoring and DFT calculations, we present a detailed view of the reaction course in the solid state. The obtained knowledge could lead to the broader application of this methodology for the deuteration of organics.

Introduction

Development of methods for direct and selective conversion of the carbon–hydrogen (C–H) bonds to the carbon–deuterium (C–D) bonds continues to be a challenge for the chemical and life sciences, as D-labeled compounds are widely used in mass spectrometry and chromatography, as well as in mechanistic and metabolic studies.[1] Moreover, such compounds can alter the ADME (absorption, distribution, metabolism, and excretion) properties of the drug.[2] The pinnacle of this is the recent approval of the first deuterated drug, deutetrabenazine, for treating chorea associated with Huntington's disease.[2,3]

Over the past 15 years, metal-catalyzed functionalization of the C–H bond has emerged as a superior approach that significantly simplifies synthesis and allows a direct hydrogen isotope exchange (HIE) in the substrate.[4a] In contrast to heterogeneously catalyzed HIE, the homogeneous metal catalysis of HIE installs D atoms at specific positions relative to the directing group.[1a,b,4a] The most frequently used metal-based catalysts for HIE of C–H bonds are Ir, Rh, Pd, and Ru compounds, whereas common deuterium sources are D-rich organic molecules, heavy water, or deuterium gas.[4]

Since most of the current homogeneous HIE reactions proceed in solutions and require high temperature, we were prompted to explore mechanochemistry as an approach to HIE. Indeed, mechanochemistry[5–9] is emerging as a sustainable and efficient synthetic approach that aims to avoid harsh reaction conditions while maintaining molecular and atomic mobility.[8] Since the reactions are carried out in the solid state, problems such as solubility or costly workup can sometimes be avoided.

In addition, mechanochemically-induced processes allow reactions at ambient temperature, often in shorter reaction time than analogous processes in solution.[6] Moreover, a recent discovery of the C–H bond activation and functionalization under mechanochemical conditions[6] enabled the preparation of stable metalated products.[7] We found it particularly interesting to use mechanochemically-prepared palladated products with the Pd-activated C–H bond(s) as precursors for the deuteration reaction. This way two steps performed in a ball mill would achieve HIE. Without using solvents and additional gaseous reactants, the deuteron source (D-source) should ideally be a molecule capable of breaking the C–Pd bond, and thereby transferring a deuteron to the carbon atom.

Here we report the first mechanochemical deuteration of the Pd-activated C(sp^2)–H bonds in various precursors (Scheme 1) and show that mechanochemical milling is a viable and efficient approach for HIE reactions. Deuteration using a deuterated L-cysteine (**Cys^{4D}**, Scheme 1) as the D-source was performed in the solid state at ambient temperature without using solvents and additional gaseous reactants. This work shows that cysteine can break the C–Pd bond and transfer a deuteron to the carbon atom. Using a simple strategy, various deuterated organic molecules were easily isolated in good to excellent yields.

Results and discussion

The deuterated L-cysteine (**Cys^{4D}**) was chosen as a D-source for the palladated precursors because it is a solid at room temperature and a readily available biologically relevant amino acid

[a]*Division of Physical Chemistry, Ruđer Bošković Institute, Bijenička 54, HR-10000, Zagreb, Croatia. E-mail: marina.juribasic@irb.hr, stipe.lukin@irb.hr*
[b]*Selvita Ltd. Zagreb, Prilaz Baruna Filipovića 29, HR-10000 Zagreb, Croatia*
†Electronic supplementary information (ESI) available. See DOI: https://doi.org/10.1039/d3qi00932g
‡These authors contributed equally to this work.

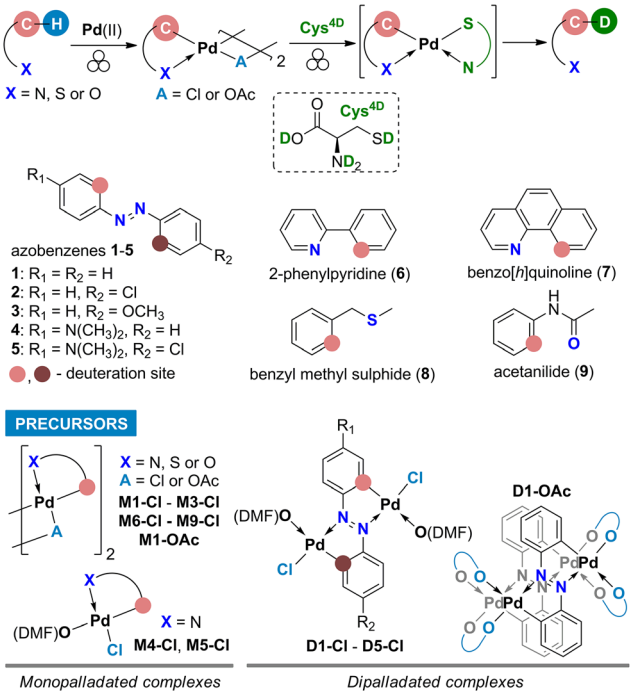

Scheme 1 General reaction route for two-step mechanochemical HIE in aromatic substrates **1–9** along with the structures of their palladated precursors.

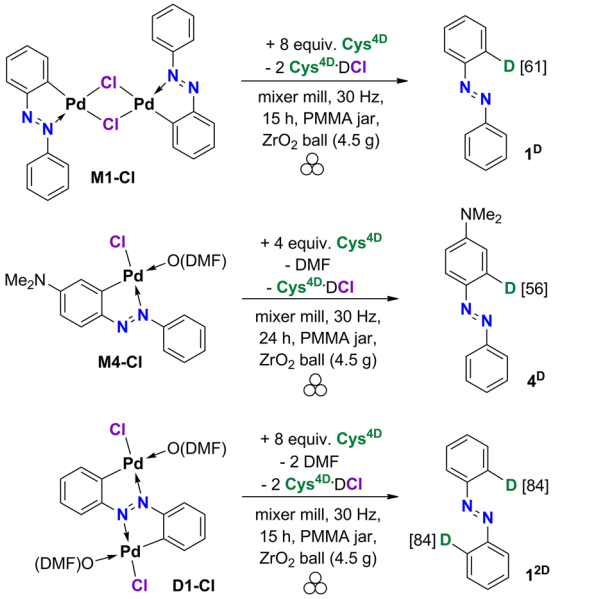

Scheme 2 Reaction conditions using three characteristic azobenzene complexes.

that coordinates strongly to the Pd centers.[10] Common inorganic D-sources (D_2O, ND_4Cl) and alcohols (ethanol-*d*) were tested and gave no deuteration whereas other deuterated solid thiols, aliphatic (1-adamantanethiol-*d*) as well as aromatic (4-chlorothiophenol-*d*), were less efficient regarding both the yield and the deuteration percentage (data in Table S1†).

For the test reactions of palladacycles with **Cys^{4D}**, we chose mono- and dicyclopalladated azobenzenes[7b,11] as precursors (**M1-Cl** and **D1-Cl**, Scheme 2). These complexes exhibit strong characteristic Raman bands[7b] allowing *in situ* Raman monitoring of their reactions which is essential for a deeper understanding of the ball-milling reaction. Namely, collected Raman data provides an insight into the reaction course as well as the nature and reactivity of the intermediates.[9]

The monopalladated precursor **M1-Cl** was reacted with **Cys^{4D}** first. The reaction proceeded nicely if an excess of **Cys^{4D}** was used. Azobenzene **1^{D}** was isolated in a 77% yield after 15 hours of milling **M1-Cl** with 4 equivalents (equiv.) of **Cys^{4D}** per palladium center (Pd). ^{1}H NMR data confirmed deuterium incorporation at the *ortho*-position to the azo group in 61% (Chart 1). To our delight, a doubly deuterated product **1^{2D}** (84%) was obtained in 83% yield by reacting **D1-Cl** with 4 equiv. of **Cys^{4D}** per Pd.

The amount of the added **Cys^{4D}** was screened on **M1-Cl** and **D1-Cl** using up to 20 equiv. of **Cys^{4D}** per Pd (Table S1†). The optimal results were obtained for 4 equiv. of **Cys^{4D}** per Pd. Thus, this ratio was further used. We note that reaction time was adjusted to maximize the yield of the isolated product.

After the successful reaction with **M1-Cl**, we applied the same methodology to unsymmetrically substituted monopalla-

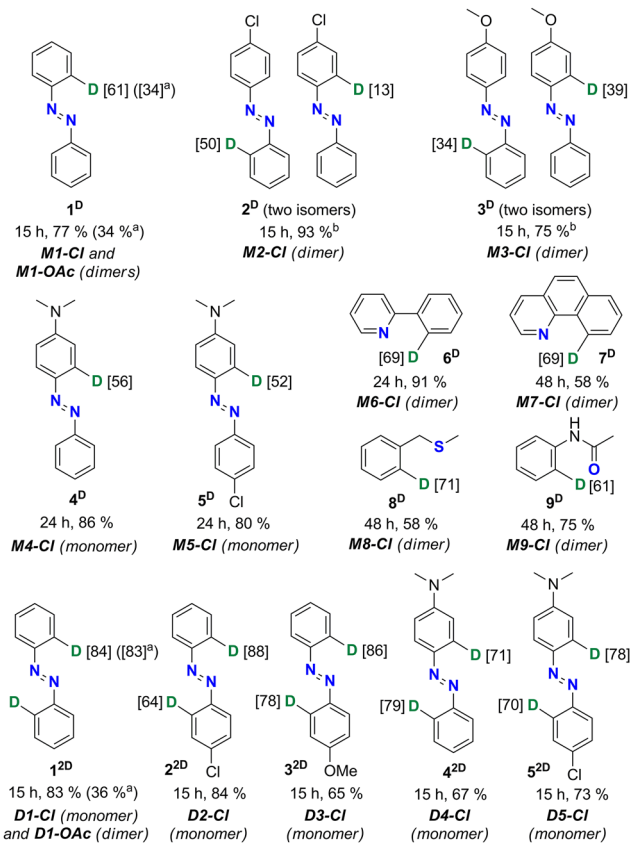

Chart 1 Products, reaction time and isolated yields of the mechanochemical deuteration of mono- and dipalladated chloride precursors (marked bellow each product in italic). Percentage of deuteration (average for all magnetically equivalent nuclei) is marked at the site of the D incorporation. [a]Data for the acetate precursors **M1-OAc** and **D1-OAc**. [b]Combined yield for two isomeric monodeuterated products.

dated azobenzenes. Milling of the dimeric monopalladated complexes of 4-chloroazobenzene (**M2-Cl**) or 4-methoxyazobenzene (**M3-Cl**) with **Cys^{4D}** led to a mixture of two monodeuterated products (**2^{D}** or **3^{D}**, Chart 1). The formation of mixtures is attributed to the presence of two isomeric forms in the precursors **M2-Cl** and **M3-Cl** (Fig. S2–S4†). In contrast, monopalladated aminoazobenzenes are monomeric precursors obtained as a single isomer in which the aminophenyl ring is palladated. Therefore, products **4^{D}** and **5^{D}** were deuterated specifically in the *ortho* position of the aminosubstituted phenyl ring by 56 and 52%, respectively (Chart 1). These experiments proved the crucial role of the substituents on the palladated substrate for determining the deuteration site, as it depends on the site of palladation.

Control reactions of the native azobenzene **1** (1 equiv.) with **Cys^{4D}** (8 equiv.) without $PdCl_2$ or with $PdCl_2$ added stoichiometrically (1 equiv.) or catalytically (5 mol%) gave no deuteration product in 15 h. Also, reactions of the precursor **D1-Cl** with glycine or L-alanine instead of **Cys^{4D}** produced dipalladated complexes in which, according to the ^{1}H NMR spectra of the reaction mixture (Fig. S52†), one molecule of the amino acid is coordinated to each Pd.

Adding an excess of D_2O (8 equiv. per Pd) to the reaction of **D1-Cl** and **Cys^{4D}** did not affect the yield or the deuteration outcome. However, adding an excess of base (8 equiv. per Pd), sodium acetate (NaOAc), or 4-(*N*,*N*-dimethylamino)pyridine (DMAP) strongly hindered the reaction ending after 15 hours of milling in traces of the isolated **1^{2D}** (Table S1†).

Deuterations of monomeric complexes **M4-Cl**, **M5-Cl**, and **D1-Cl–D5-Cl** are liquid-assisted grinding (LAG) reactions since these palladacycles contain one (**M4-Cl** and **M5-Cl**) or two (**D1-Cl–D5-Cl**) molecules of DMF that are released when **Cys^{4D}** binds to Pd. To test the DMF effect, we used the LAG reaction of the dimeric **M1-Cl** (that does not contain DMF). 1 equiv. of DMF per Pd was added to mimic the reactions of **M4-Cl** and **M5-Cl**. The isolated yield of **1^{D}** was lowered to 40%, and the deuteration percentage was 60% (compared to 61% without DMF) (Table S1†). This result can be ascribed partly to the stickier reaction mixture due to the presence of DMF and to the basic properties of DMF.

To extend our concept to other aromatics, we used chloride palladacycles of benzo[*h*]quinoline (**6**), 2-phenylpyridine (**7**), benzyl methyl sulfide (**8**), and acetanilide (**9**) containing N, S, or O donor atoms as precursors (Scheme 1). As summarized in Chart 1, our approach proved efficient allowing 61–71% single-site deuteration of these commonly used aromatics.

To explore the possibility of multiple deuteration in the same molecule, we used dipalladated azobenzenes as precursors because these compounds contain two Pd-activated C–H bonds. We were pleased to see that *ortho*-deuteration of both phenyl rings occurred, and we could isolate targets **1^{2D}–5^{2D}** in 65–84% yield (Chart 1). NMR data confirmed that D was incorporated at both sites of palladation.

Since the acetate palladated complexes are also frequently used, we attempted the deuteration using **M1-OAc** and **D1-OAc** as precursors under the same experimental conditions as for the chloride precursors. These reactions resulted in 34% and 36% yields of **1^{D}** and **1^{2D}**, respectively (Chart 1). The product **1^{D}** obtained from the acetate precursor **M1-OAc** was only 34% *ortho*-deuterated. In contrast, the deuteration of product **1^{2D}** obtained from **D1-OAc** was comparable to that of the product obtained from the reaction with the chloride precursor **D1-Cl**.

At the end of the reaction, the palladium metal is retrieved from the reaction mixture as a highly insoluble and amorphous complex with the empirical formula Pd(**Cys^{3D}**)$_2$ (see ESI† for details). Recovery of up to 85% of the elemental palladium was achieved by heating the solid Pd(**Cys^{3D}**)$_2$ above 800 °C.

Raman monitoring

To shed some light on the reaction course, we used Raman monitoring and density-functional theory (DFT) calculations.

The chloride monopalladated azobenzene (**M1-Cl**) was studied first. **M1-Cl** is a dimer with the most prominent bands in Raman spectra at 1389 and 1209 cm^{-1} belonging dominantly to ν(N=N) and ν(C–N) vibrations, respectively (Fig. 1a). These bands shift to 1380 and to 1200 cm^{-1} within 22 min of

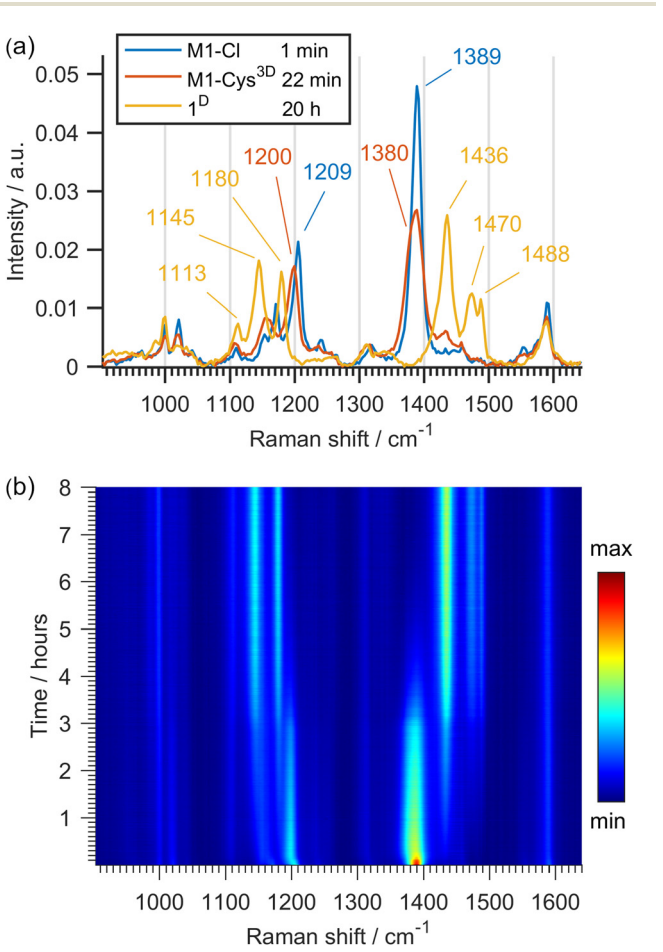

Fig. 1 (a) Selected Raman spectra and (b) 2D plot of the time-resolved Raman monitoring of the reaction of **M1-Cl** (0.14 mmol) with **Cys^{4D}** (1.12 mmol).

milling with **Cys^{4D}**, as the first intermediate **M1-1** is formed by ligand exchange in **M1-Cl** where cysteine becomes bound to Pd *via* its amino and the deprotonated thiol groups (Scheme 3). ^{1}H NMR spectrum of the reaction mixture recorded *ex situ* after 75 min of milling supports its presence (Fig. S63 and S64†). According to the DFT data, isomer **M1-1** is more stable than **M1-2**, suggesting that **M1-1** is formed in the reaction (Scheme 3).

As the reaction progressed, Raman data indicated the formation of the deuterated azobenzene **1^{D}** (Fig. 1b). Namely, bands at 1145 and 1180 cm^{-1} belonging to ν(C–N) vibrations and the bands at 1436, 1470 and 1488 cm^{-1} of ν(N=N) vibrations appeared. The final *in situ* Raman spectrum agrees with the *ex situ* data for **1^{D}** (Fig. S84†).

Raman monitoring of the reaction of **D1-Cl** with **Cys^{4D}** (Fig. 2b) revealed the presence of several intermediates preceding the formation of **1^{2D}** (Chart 1). The broad band observed in the first Raman spectrum of the reaction is at 1309 cm^{-1} and is attributed to the ν(N=N) bond of the parent compound **D1-Cl**[12a] and/or the first intermediate **D1-1** (Scheme 4). According to the DFT calculations, the Raman spectra of the starting **D1-Cl** and its planar derivative with two coordinated cysteines **D1-1** are similar, as are the spectra of **M1-Cl** and **M1-1**.

At *ca.* 30 min of milling, isomerization of **D1-1** and formation of the bridged intermediate are apparent from the emergence of a strong band at 1375 cm^{-1}, consistent with structural changes induced by the breaking of one Pd–N$_{azo}$ bond in **D1-1** and positioning of both Pd atoms on the same side of the azobenzene ligand in the bridged intermediates (Scheme 4).[12a] According to DFT calculations, two structurally similar bridged complexes **B1-1** and **B1-2**, that differ in the coordination mode of the non-bridging cysteine ligand, are most likely formed. Intensity loss and shift of the Raman band to 1389 cm^{-1} is observed after 2 hours and is related to the first deuteration and formation of **M1^{D}-2**. **M1^{D}-2** enters the second deuteration which leads to the product **1^{2D}** *ortho*-deuterated 84% (Chart 1). We note that due to the structure of the most stable isomers of **D1-1** and **B1-1**, formation of **M1^{D}-2** is predicted even though it is less stable than **M1^{D}-1**.

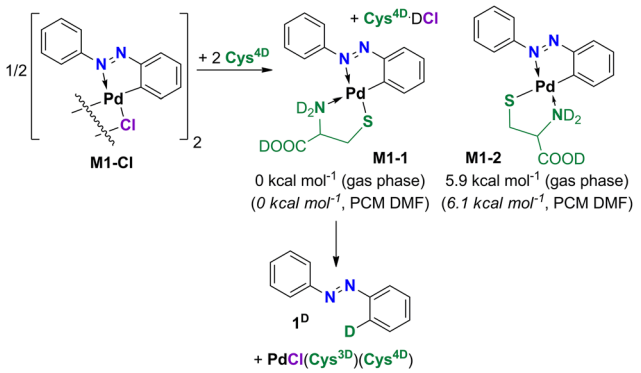

Scheme 3 Ligand exchange followed by deuteration of **M1-Cl**. **M1-2** is not formed.

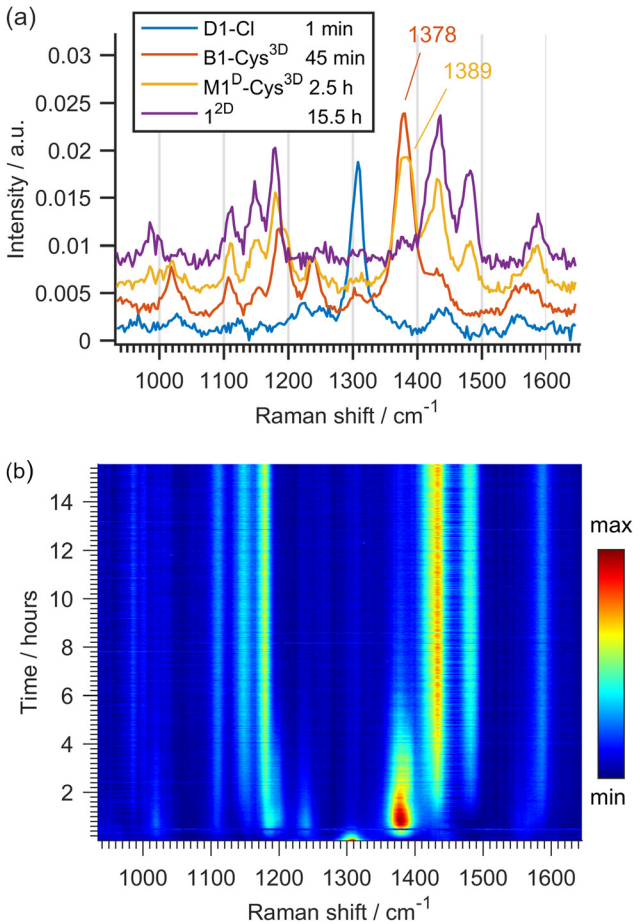

Fig. 2 (a) Selected Raman spectra and (b) 2D plot of the time-resolved Raman monitoring of the reaction of **D1-Cl** (0.14 mmol) with **Cys^{4D}** (1.12 mmol).

Isomerization of **M1^{D}-2** to **M1^{D}-1** would include breaking of the Pd–N bond and is not expected.

Insight into the dynamics of the formation of intermediates and **1^{2D}**, obtained by *in situ* Raman monitoring, shows that the second deuteration is the slowest step in the deuteration of **D1-Cl** (Fig. 2b). According to our previous work,[11,12] Raman spectra of the monopalladated complexes **M1-Cl**, **M1^{D}-1**, **M1^{D}-2** and of the bridged species **B1-1** and **B1-2** are remarkably similar. However, the higher observed consumption rate of the bridged dipalladated complex than of the monopalladated complex allowed us to distinguish their ν(N=N) bands at 1378 and 1389 cm^{-1}, respectively, and thus to characterize each deuteration step.

DFT calculations

In situ and *ex situ* monitoring suggested a complex reaction route to the deuterated products but could not determine which of the available D-sources would most likely engage in the reaction. Moreover, Raman data gave limited information about the involved reaction intermediates for **D1-Cl**. We thus modeled the deuteration of mono- and dipalladated azobenzene precursors.

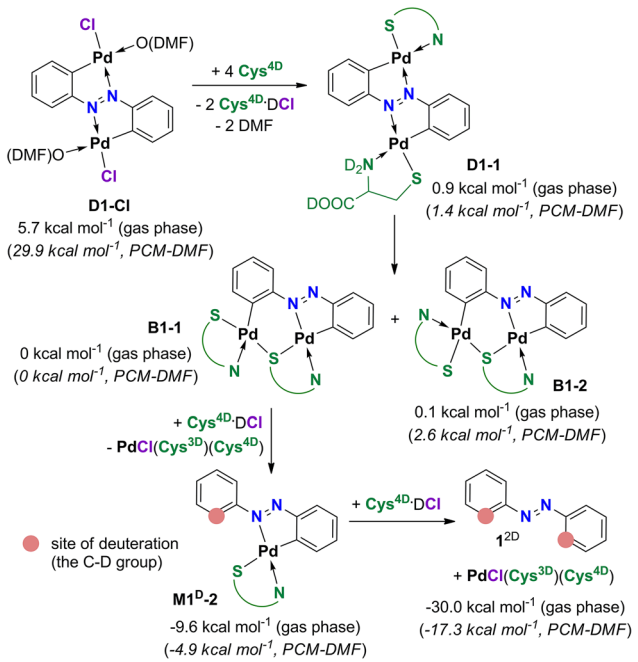

Scheme 4 Proposed reaction route from **D1-Cl** to $\mathbf{1}^{2D}$.

D-source. The first and experimentally observed step of the deuteration is the anion exchange (chloride or acetate) with $\mathbf{Cys}^{4D}$ yielding cysteine complexes **M1-1** (Scheme 3) or **D1-1** (Scheme 4). Calculated data agree with the cysteine complexes being more stable than chloride or acetate precursors. An acid (DCl or AcOD) is released during this process. In addition, the formation of cysteine deuterochloride ($\mathbf{Cys}^{4D}$·DCl) is expected for the chloride precursors. Hence, DCl or AcOD, $\mathbf{Cys}^{4D}$, or $\mathbf{Cys}^{4D}$·DCl could act as D-sources. In addition, ND_3^+ COOD and SD groups in deuterated cysteine might be involved in the D-transfer.

After elaborate analysis of the possible options for the deuteration of the monopalladated azobenzenes **M1-1** (Fig. 3) and **M1-2** (Table S3†), $\mathbf{Cys}^{4D}$·DCl was identified as the preferred D-source for the deuteration of the chloride precursors, whereas $\mathbf{Cys}^{4D}$ is the D-source for the acetate precursors and at the beginning of the reaction. Calculations show that both ND_3^+ and COOD groups can deuterate the palladated ligand. The preference for one over the other depends on the intra- and intermolecular interactions near the deuteration site and is mainly on the side of the COOD as a donor group.

Deuteration of the monopalladated azobenzene. Out of two possible isomers for the monopalladated cysteine complex (Fig. 3), a more stable **M1-1** is formed and deuterated to $\mathbf{1}^{D}$.

The calculated free-energy profile for the deuteration of **M1-1** by various D-sources (Fig. 3) agrees with the experimental findings. Deuteration by $\mathbf{Cys}^{4D}$·DCl is a less energy-demanding than deuteration using $\mathbf{Cys}^{4D}$ as a D-source. The lowest-lying transition states for deuteration of **M1-1** are at 9.8 kcal mol^{-1} for $\mathbf{Cys}^{4D}$·DCl and at 17.5 kcal mol^{-1} for $\mathbf{Cys}^{4D}$, which agrees with the reaction of **M1-Cl** being faster than the reaction using **M1-OAc** as the precursor.

Deuteration of the dipalladated azobenzene. Isomerization of **D1-1** formed by the reaction of **D1-Cl** and $\mathbf{Cys}^{4D}$ gives an *S*-bridged cysteine dipalladated complex likely present in two isomeric forms **B1-1** and **B1-2** (Scheme 4). Both can be involved in the D-transfer. Gas-phase stabilities of these two isomers are almost equal, but after optimization using PCM-DMF to check for the medium influence on their stability, **B1-2** was calculated to be less stable than **B1-1** and also **D1-1**. Other possible bridged isomers are much less stable and thus are not formed (Scheme S2†). Thus, **B1-1** should be the form of the dipalladated complex that preferentially enters the first D-transfer.

In the *S*-bridged dipalladated cysteine complexes, the five- and six-membered palladated rings have to be deuterated to obtain $\mathbf{1}^{2D}$, Scheme 5. Two paths can be envisaged depending on which ring is broken first, and both were considered. Both paths end in the doubly *ortho*-palladated $\mathbf{1}^{2D}$.

In path I, the phenyl group involved in the six-membered palladated ring of the *S*-bridged dipalladated complex is deuterated first, Scheme 6. Following this path, **B1-1** transforms to the monodeuterated intermediate $\mathbf{M1}^{D}$-2 with the conserved

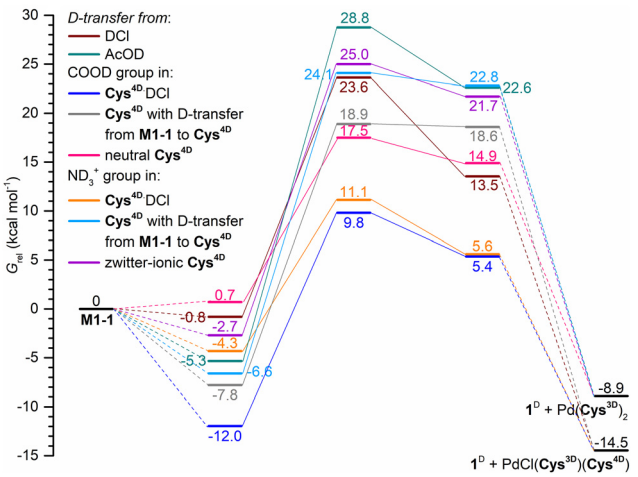

Fig. 3 D-transfer to **M1-1** from various D-sources. B3LYP-D3/6-311+G**/SDD(Pd)/gas phase free energies reported relative to **M1-1** (in kcal mol^{-1}).

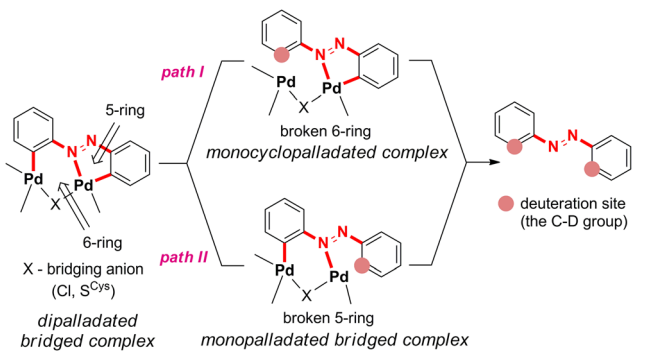

Scheme 5 Paths leading from the dipalladated complex to the dideuterated azobenzene.

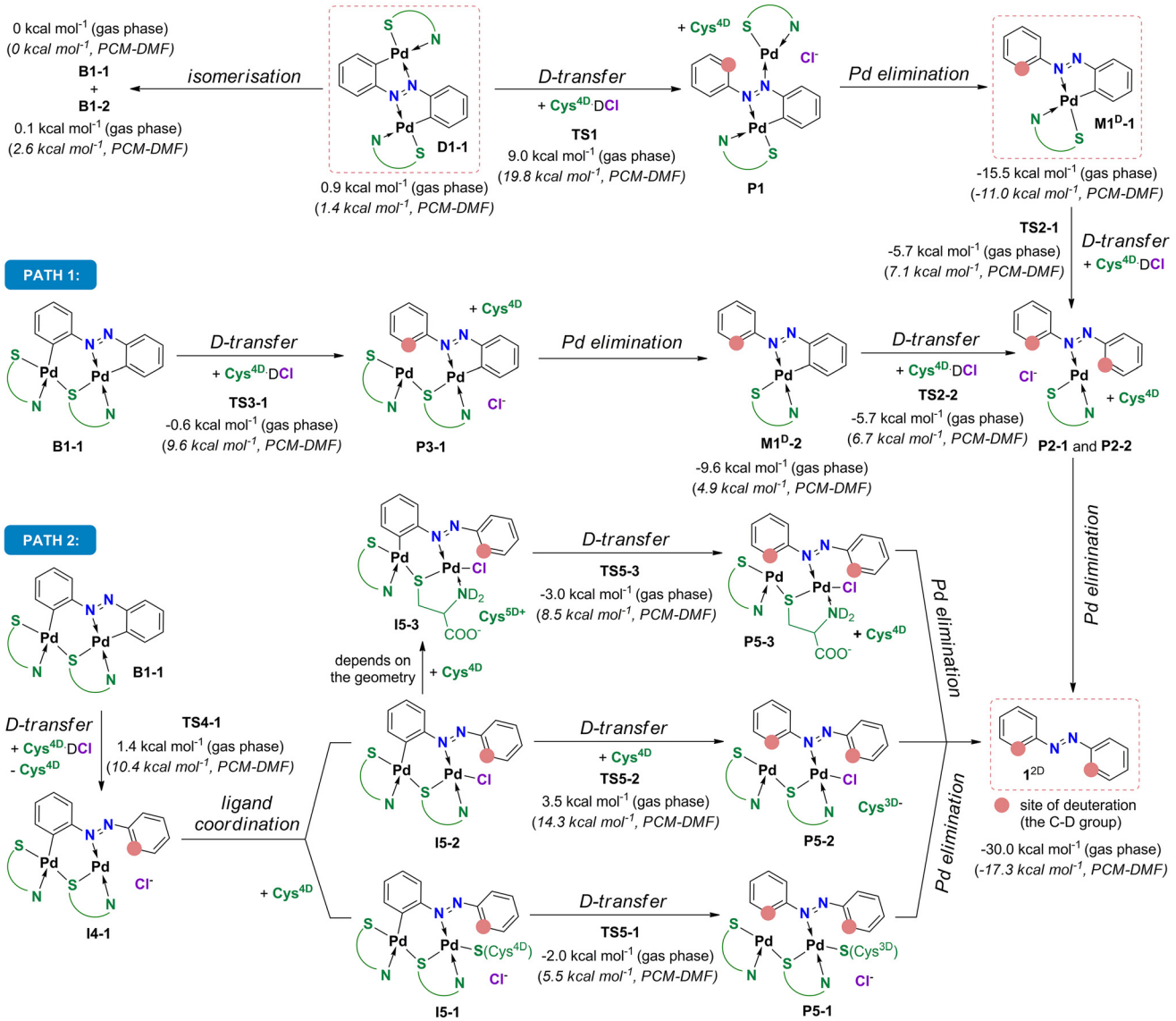

Scheme 6 Deuteration of **B1-1** by **Cys^{4D}**·DCl to **1^{2D}** following path I and path II. Experimentally characterized compounds are highlighted in dashed rectangles.

five-membered cyclopalladated ring *via* transition state **TS3-1**. After the elimination of one palladium center, **M1^{D}-2** undergoes the second deuteration that breaks the five-membered ring to give **1^{2D}** after Pd elimination.

Path II starts with the deuteration of the five-membered cyclopalladated ring in the *S*-bridged dipalladated complex, Scheme 6. Monopalladated *S*-bridged intermediate with one empty coordination place (**I4-1**) is formed. **Cys^{4D}** or chloride can fill this place and form complexes **I5-1** or **I5-2**, respectively. In addition, **I5-2** can be deprotonated in presence of **Cys^{4D}** and form ion pair **I5-3**. This process is spontaneous for the tested geometries both in the gas phase and using the PCM model for DMF. All three species (**I5-1–I5-3**) can enter the second D-transfer and after Pd elimination form **1^{2D}**.

The first step of the path I is less energy-demanding than the first step of the path II for **B1-1** (Fig. 4) and **B1-2** (Fig. S138†). Deuteration of the planar **D1-1** is the most energetically-demanding process that would occur *via* transition state **TS1** located *ca.* 10 kcal mol^{-1} higher in energy than transition states **TS3-1** and **TS3-2** in the path I and is thus not expected to occur. Therefore, the path I is preferred.

Calculations using other methods. Presented data was obtained using the B3LYP-D3/6-311+G**/SDD(Pd) level of theory in the gas phase. Other functionals (B3LYP and ωB97x-D) and basis sets (6-31G*/SDD(Pd) and def2tzvp) were also evaluated by modeling the deuteration of **M1-1** (Table S2†). D-transfer from **Cys^{4D}**·DCl to **M1-1** is preferred for all methods. Free energies of the transition states for D-transfer by various D-sources increase in the order: **Cys^{4D}**·DCl < **Cys^{4D}** < DCl < AcOD.

To account for the possible influence of the reaction medium, we have used the B3LYP-D3/6-311+G**/SDD(Pd)

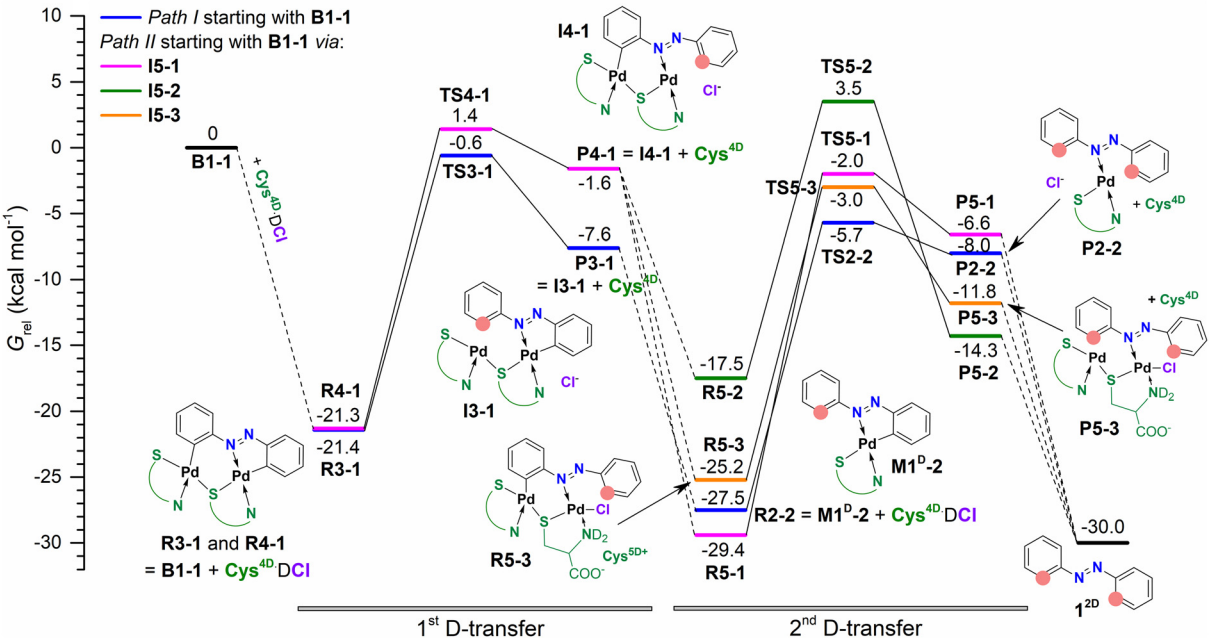

Fig. 4 Free-energy profile for deuteration of **B1-1** by **Cys^{4D}**·DCl to **1^{2D}**. B3LYP-D3/6-311+G**/SDD(Pd)/gas phase data (in kcal mol^{-1}) reported relative to **B1-1**. Palladium is eliminated as PdCl(**Cys^{3D}**)(**Cys^{4D}**).

level of theory with PCM modeling of propanoic acid (ε = 3.44) and DMF (ε = 37.22) as solvents. We note that the examined reaction mixtures might likely have a lower dielectric constant than DMF and thus, PCM-DMF data should be regarded as a guide for how a polar medium can influence the reaction.

Data obtained by PCM calculations for deuteration of **M1-1** show that the difference in the free energies of the transition states for the D-transfer by **Cys^{4D}**·DCl and **Cys^{4D}** got smaller as the medium polarity increased (Table S2 and Fig. S136†). This difference is 7.7 kcal mol^{-1} in the gas phase (free energies of the transition states are 9.8 kcal mol^{-1} for **Cys^{4D}**·DCl and 17.5 kcal mol^{-1} for **Cys^{4D}**, Fig. 3), 4.8 kcal mol^{-1} in the propanoic acid (14.2 for **Cys^{4D}**·DCl and 19.0 kcal mol^{-1} for **Cys^{4D}**), and 0.3 kcal mol^{-1} in DMF (18.1 kcal mol^{-1} for **Cys^{4D}**·DCl and 18.4 kcal mol^{-1} for **Cys^{4D}**). Results suggest that **Cys^{4D}**, along with the still preferred **Cys^{4D}**·DCl, might also act as a D-source for deuteration in DMF.

To further test the presented results in the gas phase, we have performed PCM-DMF calculations for the deuteration of **D1-Cl** (Fig. S138†). Free energies of the reactants, transition states and products are lifted relative to **B1-1**. General trend that was observed in the gas phase is preserved in DMF. Data agree with the facile reaction that still shows a small preference to the path I leading from **D1-Cl** to **1^{2D}**.

In the gas phase PdCl(**Cys^{3D}**)(**Cys^{4D}**) is by 5.5 kcal mol^{-1} more stable than the monomeric form of Pd(**Cys^{3D}**)$_2$ (Chart S1†). However, Pd(**Cys^{3D}**)$_2$ is preferred by 1.0 and 6.1 kcal mol^{-1} in propanoic acid and DMF, respectively. Thus, PdCl(**Cys^{3D}**)(**Cys^{4D}**) could form during reaction and change to the isolated solid Pd(**Cys^{3D}**)$_2$ during work-up.

Experimental

Experimental details, spectral data for new compounds, *in situ* Raman experiments and additional computational data and details can be found in the ESI.†

Ball-milling reactions

Experiments were performed using an IST500 mixer mill operating at 30 Hz with a built-in fan. Deuteration of precursors was carried out sequentially under analogous conditions at an ambient temperature of 22 ± 2 °C. These reactions were performed in transparent 14 mL poly(methyl methacrylate (PMMA) jars that allowed *in situ* Raman monitoring. One milling ball made of zirconium(IV)oxide (ZrO_2, 12 mm, 4.5 g) was used. Reactions were performed using approximately 225 mg of the reaction mixture.

In situ Raman monitoring without interrupting the milling process was performed using a portable Raman system with PD-LD (now Necsel) BlueBox laser source with an excitation wavelength of 785 nm, equipped with a B&W-Tek BAC102 fiber-optic Raman probe and coupled to OceanOptics Maya2000Pro spectrometer. The most intense band of the PMMA vessel at 2955 cm^{-1}, corresponding to the ν(C–H) bond, was used as a scaling reference to subtract its contribution from the experimental Raman spectra. The asymmetric least squares (AsLS) method[13a] was used to correct the spectra baseline. To extract the spectra of observed species, multivariate curve resolution with alternative least squares method (MCR-ALS)[13b] in MATLAB was used. The literature data[14] and quantum chemical calculations were used to assign experimental spectra.

Deuteration of precursors

0.14 mmol of the dimeric monopalladated (**M1-Cl–M3-Cl**, **M6-Cl–M9-Cl**, **M1-OAc**) or the monomeric dipalladated complexes (**D1-Cl–D5-Cl**, **D1-OAc**) was milled with 1.12 mmol of **Cys^{4D}** (4 equiv. per Pd). 0.28 mmol of the precursor and 1.12 mmol of **Cys^{4D}** (4 equiv. per Pd) were used in reactions of the monomeric monopalladated complexes (**M4-Cl** and **M5-Cl**). Completeness of the reactions was confirmed by *in situ* Raman monitoring and *ex situ* ^{1}H NMR spectra of the reaction mixtures. No change in the reaction mixture was observed after milling was stopped. Reaction duration, isolated yields, and deuteration site and the appropriate percentage are given in Chart 1.

Deuteration of thiols

3.0 g of native L-**Cys** was dissolved in 16 mL of D_2O. The solution was refluxed for 1 h, evaporated under reduced pressure, and cooled to ambient temperature. This procedure was repeated twice each time using a new portion of D_2O. The deuteration was confirmed by IR and Raman spectroscopies (Fig. S83, S91 and S92†).

1.0 g of native 1-adamantanethiol or 4-chlorothiophenol was dissolved in 15 mL ethanol-*d* (EtOD). The solution was refluxed for 1 h, evaporated under reduced pressure, and cooled to ambient temperature. This procedure was repeated twice each time using a new portion of EtOD. The deuteration was confirmed by IR and ^{1}H NMR spectroscopies (Fig. S17, S18, S93 and S94†).

DFT calculations

Calculations were carried out in Gaussian16[15] using a functional with Grimme's empirical correction (B3LYP-D3).[16] Pd atoms were modeled by the Stuttgart–Dresden (SDD) pseudopotential and the accompanying SDD basis set.[17] Standard 6-311+G** basis set was used for C, H/D, N, O, S and Cl atoms. Other functionals (ωB97x-D,[18] B3LYP), basis sets (6-31G*/SDD (Pd) and def2tzvp) and polarizable continuum modeling[19] (DMF and propanoic acid) were also tested (see Table S2†). Full geometry optimizations were accompanied by vibrational frequency calculations that identified calculated stationary points as minima (reactants and products) or first-order saddle points (transition states). Nature of the transition states was confirmed by intrinsic reaction coordinate (IRC) searches[20] followed by full geometry optimizations. Reported energies are free energies given at 298.15 K and 1 atm. No additional corrections were applied. Data for deuteration of the mono- and dipalladated azobenzene are reported relative to **M1-1** and **B1-1**, respectively.

Conclusions

We have developed a novel approach for the deuteration of C(sp^2)–H bonds by reacting palladacycles with **Cys^{4D}** in a ball mill at ambient temperature and without solvents. The advantage of this simple approach is that the reactions are carried out in the solid state, thus avoiding solubility problems and undesirable solvent effects. The incorporation of one or two deuterons at predictable sites of structurally diverse aromatics makes this method practical and offers a fresh approach to an old demand. The presented work thus paves the way for similar concepts for solid-state hydrogen exchange reactions that could be extended to various transition metals and substrates with sp^2 and sp^3 C–H bonds, which will be the focus of our future work.

Conflicts of interest

There are no conflicts to declare.

Acknowledgements

Financial support was provided by the Croatian Science Foundation (grants IP-2019-04-9951 and IP-2020-02-1419). Computations were done on the Isabella cluster at SRCE, Zagreb, Croatia. We thank Dr Darko Babić for his valuable assistance and discussion, Dr Tatjana Šumanovac and Dr Senada Muratović for experimental help, and Dr Sunčica Roca and Ms NIkolina Višić for a part of the NMR measurements.

References

1 (*a*) J. Atzrodt and V. Derdau, Pd- and Pt-catalyzed H/D exchange methods and their application for internal MS standard preparation from a Sanofi-Aventis perspective, *J. Labelled Compd. Radiopharm.*, 2010, **53**, 674–685; (*b*) J. Atzrodt, V. Derdau, T. Fey and J. Zimmermann, The Renaissance of H/D Exchange, *Angew. Chem., Int. Ed.*, 2007, **46**, 7744–7765; (*c*) J. Yang, *Deuterium: Discovery and Applications in Organic Chemistry*, Elsevier, Amsterdam, 2016; (*d*) J. Atzrodt, V. Derdau, W. J. Kerr and M. Reid, Deuterium- and Tritium-Labelled Compounds: Applications in the Life Sciences, *Angew. Chem., Int. Ed.*, 2018, **57**, 1758–1784; (*e*) G. C. Lloyd-Jones and M. P. Muñoz, Isotopic labelling in the study of organic and organometallic mechanism and structure: an account, *J. Labelled Compd. Radiopharm.*, 2007, **50**, 1072–1087; (*f*) S. A. Blum, K. L. Tan and R. G. Bergman, Application of Physical Organic Methods to the Investigation of Organometallic Reaction Mechanisms, *J. Org. Chem.*, 2003, **68**, 4127–4137; (*g*) M. Gómez-Gallego and M. A. Sierra, Kinetic Isotope Effects in the Study of Organometallic Reaction Mechanisms, *Chem. Rev.*, 2011, **111**, 4857–4963.

2 T. Pirali, M. Serafini, S. Cargnin and A. A. Genazzani, Applications of Deuterium in Medicinal Chemistry, *J. Med. Chem.*, 2019, **62**, 5276–5297.

3 C. Schmidt, First deuterated drug approved, *Nat. Biotechnol.*, 2017, **35**, 493–494.

4 (*a*) J. Atzrodt, V. Derdau, W. J. Kerr and M. Reid, C–H Functionalisation for Hydrogen Isotope Exchange, *Angew. Chem., Int. Ed.*, 2018, **57**, 3022–3047; (*b*) W. J. Kerr, D. M. Lindsay, P. K. Owens, M. Reid, T. Tuttle and S. Campos, Site-Selective Deuteration of *N*-Heterocycles via Iridium-Catalyzed Hydrogen Isotope Exchange, *ACS Catal.*, 2017, **7**, 7182–7186; (*c*) S. Chen, G. Song and X. Li, Chelation-assisted rhodium hydride-catalyzed regioselective H/D exchange in arenes, *Tetrahedron Lett.*, 2008, **49**, 6929–6932; (*d*) H. Xu, M. Liu, L.-J. Li, Y.-F. Cao, J.-Q. Yu and H.-X. Dai, Palladium-Catalyzed Remote *meta*-C–H Bond Deuteration of Arenes Using a Pyridine Template, *Org. Lett.*, 2019, **21**, 4887–4891; (*e*) L. Piola, J. A. Fernandez-Salas, S. Manzini and S. P. Nolan, Regioselective ruthenium catalysed H–D exchange using D_2O as the deuterium source, *Org. Biomol. Chem.*, 2014, **12**, 8683–8688.

5 (*a*) S. L. James, C. J. Adams, C. Bolm, D. Braga, P. Collier, T. Friščić, F. Grepioni, K. D. M. Harris, G. Hyett, W. Jones, A. Krebs, J. Mack, L. Maini, A. G. Orpen, I. P. Parkin, W. C. Shearouse, J. W. Steed and D. C. Waddell, Mechanochemistry: opportunities for new and cleaner synthesis, *Chem. Soc. Rev.*, 2012, **41**, 413–417; (*b*) T. Friščić, Supramolecular concepts and new techniques in mechanochemistry: cocrystals, cages, rotaxanes, open metal-organic frameworks, *Chem. Soc. Rev.*, 2012, **41**, 3493–3510; (*c*) G.-W. Wang, Mechanochemical organic synthesis, *Chem. Soc. Rev.*, 2013, **42**, 7668–7700; (*d*) D. Braga, L. Maini and F. Grepioni, Mechanochemical preparation of co-crystals, *Chem. Soc. Rev.*, 2013, **42**, 7638–7648; (*e*) N. R. Rightmire and T. P. Hanusa, Advances in organometallic synthesis with mechanochemical methods, *Dalton Trans.*, 2016, **45**, 2352–2362.

6 (*a*) A. Porcheddu, E. Colacino, L. De Luca and F. Delogu, Metal-Mediated and Metal-Catalyzed Reactions under Mechanochemical Conditions, *ACS Catal.*, 2020, **10**, 8344–8394; (*b*) J. G. Hernández and C. Bolm, Altering Product Selectivity by Mechanochemistry, *J. Org. Chem.*, 2017, **82**, 4007–4019; (*c*) J. G. Hernandez, C–H Bond Functionalization by Mechanochemistry, *Chem. – Eur. J.*, 2017, **23**, 17157–17165; (*d*) S. Zhao, Y. Li, C. Liu and Y. Zhao, Recent advances in mechanochemical C–H functionalization reactions, *Tetrahedron Lett.*, 2018, **59**, 317–324.

7 (*a*) M. Juribašić, K. Užarević, D. Gracin and M. Ćurić, Mechanochemical C–H bond activation: rapid and regioselective double cyclopalladation monitored by *in situ* Raman spectroscopy, *Chem. Commun.*, 2014, **50**, 10287–10290; (*b*) A. Bjelopetrović, S. Lukin, I. Halasz, K. Užarević, I. Đilović, D. Barišić, A. Budimir, M. Juribašić Kulcsár and M. Ćurić, Mechanism of Mechanochemical C–H Bond Activation in an Azobenzene Substrate by Pd^{II} Catalysts, *Chem. – Eur. J.*, 2018, **24**, 10672–10682; (*c*) D. Barišić, I. Halasz, A. Bjelopetrović, D. Babić and M. Ćurić, Mechanistic Study of the Mechanochemical Pd^{II}-Catalyzed Bromination of Aromatic C–H Bonds by Experimental and Computational Methods, *Organometallics*, 2022, **41**, 1284–1294; (*d*) D. Barišić, M. Pajić, I. Halasz, D. Babić and M. Ćurić, Mechanochemical halogenation of unsymmetrically substituted azobenzenes, *Beilstein J. Org. Chem.*, 2022, **18**, 680–687.

8 S. Lukin, M. Tireli, T. Stolar, D. Barišić, M. V. Blanco, M. Di Michiel, K. Užarević and I. Halasz, Isotope Labeling Reveals Fast Atomic and Molecular Exchange in Mechanochemical Milling Reactions, *J. Am. Chem. Soc.*, 2019, **141**, 1212–1216.

9 (*a*) S. Lukin, L. Germann, T. Friščić and I. Halasz, Toward Mechanistic Understanding of Mechanochemical Reactions Using Real-Time *In Situ* Monitoring, *Acc. Chem. Res.*, 2022, **55**, 1262–1277; (*b*) S. Lukin, K. Užarević and I. Halasz, Raman spectroscopy for *real-time* and *in situ* monitoring of mechanochemical milling reactions, *Nat. Protoc.*, 2021, **16**, 3492–3521.

10 (*a*) N. Yoshinari, N. Kuwamura, T. Kojima and T. Konno, Development of coordination chemistry with thiol-containing amino acids, *Coord. Chem. Rev.*, 2023, **474**, 214857; (*b*) V. K. Jain and L. Jain, The chemistry of tri- and high-nuclearity palladium(II) and platinum(II) complexes, *Coord. Chem. Rev.*, 2010, **254**, 2848–2903.

11 (*a*) M. Juribašić, A. Budimir, S. Kazazić and M. Ćurić, Dicyclopalladated Complexes of Asymmetrically Substituted Azobenzenes: Synthesis, Kinetics and Mechanisms, *Inorg. Chem.*, 2013, **52**, 12749–12757; (*b*) A. Bjelopetrović, M. Robić, D. Babić, M. Juribašić Kulcsár and M. Ćurić, Facile Mechanochemical Anion Substitution in Cyclopalladated Azobenzenes, *Organometallics*, 2019, **38**, 4479–4484; (*c*) A. Bjelopetrović, D. Barišić, Z. Duvnjak, I. Džajić, M. Juribašić Kulcsár, I. Halasz, M. Martinez, A. Budimir, D. Babić and M. Ćurić, A Detailed Kinetico-Mechanistic Investigation on the Palladium C–H Bond Activation in Azobenzenes and Their Monopalladated Derivatives, *Inorg. Chem.*, 2020, **59**, 17123–17133.

12 (*a*) M. Juribašić Kulcsár, I. Halasz, A. Budimir, K. Užarević, S. Lukin, A. Monas, F. Emmerling, J. Plavec and M. Ćurić, Reversible Gas-Solid Ammonia N–H Bond Activation Mediated by an Organopalladium Complex, *Inorg. Chem.*, 2017, **56**, 5342–5351; (*b*) M. Juribašić, I. Halasz, D. Babić, D. Cinčić, J. Plavec and M. Ćurić, Aging and Ball-Milling as Low-Energy and Environmentally Friendly Methods for the Synthesis of Pd(II) Photosensitizers, *Organometallics*, 2014, **33**, 1227–1234.

13 (*a*) P. H. C. Eilers and H. F. M. Boelens, *Baseline Correction with Asymmetric Least Squares Smoothing*, Leiden University Medical Center Report, 2015; (*b*) J. Jaumot, A. de Juan and R. Tauler, MCR-ALS GUI 2.0: New features and applications, *Chemom. Intell. Lab. Syst.*, 2015, **140**, 1–12.

14 (*a*) N. Biswas and S. Umapathy, Structures, Vibrational Frequencies, and Normal Modes of Substituted Azo Dyes: Infrared, Raman, and Density Functional Calculations, *J. Phys. Chem. A*, 2000, **104**, 2734–2745; (*b*) G. Socrates, *Infrared and Raman Characteristic Group Frequencies*, J. Wiley & Sons, Chichester, 3rd edn, 2001.

15 M. J. Frisch, G. W. Trucks, H. B. Schlegel, G. E. Scuseria, M. A. Robb, J. R. Cheeseman, G. Scalmani, V. Barone, G. A. Petersson, H. Nakatsuji, X. Li, M. Caricato, A. V. Marenich, J. Bloino, B. G. Janesko, R. Gomperts, B. Mennucci, H. P. Hratchian, J. V. Ortiz, A. F. Izmaylov, J. L. Sonnenberg, D. Williams-Young, F. Ding, F. Lipparini, F. Egidi, J. Goings, B. Peng, A. Petrone, T. Henderson, D. Ranasinghe, V. G. Zakrzewski, J. Gao, N. Rega, G. Zheng, W. Liang, M. Hada, M. Ehara, K. Toyota, R. Fukuda, J. Hasegawa, M. Ishida, T. Nakajima, Y. Honda, O. Kitao, H. Nakai, T. Vreven, K. Throssell, J. A. Montgomery Jr., J. E. Peralta, F. Ogliaro, M. J. Bearpark, J. J. Heyd, E. N. Brothers, K. N. Kudin, V. N. Staroverov, T. A. Keith, R. Kobayashi, J. Normand, K. Raghavachari, A. P. Rendell, J. C. Burant, S. S. Iyengar, J. Tomasi, M. Cossi, J. M. Millam, M. Klene, C. Adamo, R. Cammi, J. W. Ochterski, R. L. Martin, K. Morokuma, O. Farkas, J. B. Foresman and D. J. Fox, *Gaussian 16, Revision C.01*, Gaussian, Inc., Wallingford, CT, 2016.

16 (*a*) P. J. Stephens, F. J. Devlin, C. F. Chabalowski and M. J. Frisch, Ab Initio Calculation of Vibrational Absorption and Circular Dichroism Spectra Using Density Functional Force Fields, *J. Phys. Chem.*, 1994, **98**, 11623–11627; (*b*) S. Grimme, J. Antony, S. Ehrlich and H. Krieg, A consistent and accurate ab initio parametrization of density functional dispersion correction (DFT-D) for the 94 elements H-Pu, *J. Chem. Phys.*, 2010, **132**, 154104.

17 D. Andrae, U. Haussermann, M. Dolg, H. Stoll and H. Preuss, Energy-adjusted *ab initio* pseudopotentials for the second and third row transition elements, *Theor. Chim. Acta*, 1990, **77**, 123–141.

18 J.-D. Chai and M. Head-Gordon, Long-range corrected hybrid density functionals with damped atom–atom dispersion corrections, *Phys. Chem. Chem. Phys.*, 2008, **10**, 6615–6620.

19 S. Miertuš, E. Scrocco and J. Tomasi, Electrostatic interaction of a solute with a continuum. A direct utilization of *ab initio* molecular potentials for the prevision of solvent effects, *Chem. Phys.*, 1981, **55**, 117–129.

20 K. Fukui, The path of chemical reactions - the IRC approach, *Acc. Chem. Res.*, 1981, **14**, 363–368.

